Journal of Electrical Engineering & Technology (2023) 18:1693–1704
https://doi.org/10.1007/s42835-022-01312-y

ORIGINAL ARTICLE

A Synchrophasor-Based Line Protection for Single Phase-Ground Faults

N. V. Phanendra Babu[1] · P. Suresh Babu[2] · Saptarshi Roy[3] · T. Sudhakar Babu[1] · Anil Bharadwaj[4]

Received: 23 November 2021 / Revised: 17 September 2022 / Accepted: 8 November 2022 / Published online: 27 November 2022

Abstract
Synchrophasor measurement data enhances the transmission line protection. This paper proposes an improved line protection against single phase-ground faults using synchronized phasor data. This algorithm prevents the relay mal-operation caused by high fault resistance. This algorithm calculates the phase difference between relay point voltage and fault point voltage based on the relation between negative sequence of relay point current and fault point current. After, the calculated phase difference between relay point voltage and fault point voltage will be compared with set point voltage phase referred from the relay point voltage phase. The fault detection action will be taken according to a certain phase difference relation between fault point voltage and set point voltage. This method is then applied to a practical single machine single line system. The results show that the suggested algorithm could determine in-line faults accurately with less computational time. It also has proved that this method is immune to the fault resistance, system conditions.

Keywords Single line-ground faults · Synchronized phasor measurement data · Relay point voltage · Fault point voltage · Phase angle · Fault resistance · Inception angle

1 Introduction

In power systems, single line-ground faults are the most frequent faults. Particularly, if a single line-ground fault occurs with fault resistance, it may mal-operate the relays protecting that particular zone. Sometimes, this causes an unnecessary tripping of healthy lines, and it may lead to cascading failure. So, an extensive research is required to be done in the area of power system protection. Initially, a two end phasor estimation based line protection algorithm is introduced in [1]. Later, a fault detection index based algorithm [2–4] is suggested. In [5–10], synchronized voltage and current measurements obtained from the both ends of a line were used to determine the fault. Considering arcing, fault location algorithm was proposed in [11, 12]. Later, authors found that the decaying D.C. component present in transient current is having a significant effect in estimating the fault [13, 14]. So, authors propose an algorithm for removing decaying D.C component to detect faults in the transmission system accurately in [15]. After, a mimic filter is designed to remove the D.C. offset [16]. A method based on the recursive relation between even and odd samples was proposed in [17] to develop a modified DFT algorithm to identify faults. Later, an iterative current filtering technique is suggested in [18]. Even though all these methods were accurate enough, they were compromised with time because of their complexity. Moreover, they haven't suggested any idea to improve the immunity of protection algorithm to the resistance involved faults. Later, [19, 20] outline a fault detection method for resistance faults by compensating resistance calculated from

✉ N. V. Phanendra Babu
phanendrababu_eee@cbit.ac.in

✉ T. Sudhakar Babu
sudhakarbabu66@gmail.com

P. Suresh Babu
drsureshperli@nitw.ac.in

Saptarshi Roy
saptarshi.roy.ju@gmail.com

Anil Bharadwaj
anilbharadwajc@gmail.com

[1] Department of Electrical and Electronic Engineering, CBIT, Hyderabad, India

[2] Electrical Engineering Department, NIT Warangal, Warangal, India

[3] Department of Electrical and Electronic Engineering, Mirmadan Mohanlal Government Polytechnic, Plassey, WB, India

[4] Department of Electrical Engineering, IIT Kharagpur, Kharagpur, WB, India

the power at relaying point. Next, high-resistance faults are identified by differentiating the active power flow [21]. Recently, by calculating the real power drawn by the fault resistance the in-line fault has been found [22]. Authors [23, 24] have improved the immunity of protection by adjusting the relay setting values. But, all the above methods haven't used the voltage phasor data for their analysis even though they have succeeded in detecting the ground faults involving fault resistance.

Very recently, a line protection method is proposed by comparing the voltage phasors [25]. But significantly, this method has not considered synchronized data for its estimation. The synchrophasor measurement data enhances the transmission line protection to very greater extent [26–29]. Unlike above methods, the proposed paper aims at identifying the ground faults involving high fault resistance using synchronized voltage phasor data from the relaying point. This scheme calculates the phase difference between relay point voltage and fault point voltage based on the relation between negative sequence of relay point current and fault point current. After, to identify fault existence in the line, the calculated phase difference between relay point voltage and fault point voltage will be compared with the set point voltage phase referred from relay point voltage phase.

The paper is well organized as stion II gives the clear idea about the fault identification methodology. Stion III discusses the effectiveness of this technique by showing the results. Stion IV concludes the papers.

2 Proposed Phase Comparison Technique

2.1 Single-Sourced System

Let us consider the system as shown in Fig. 1. E_g is the source voltage estimated by the PMU placed at relay point r. And, z_g is the source impedance, z_{set} is the set-point (or zone) impedance which is for the portion of the line Rs, z_{line} is the total line impedance.

For a single-phase to ground fault at a point *f,* the sequence network becomes as shown in Fig. 2. As shown in Fig. 2, the fault sequence currents i_{f1}, i_{f2}, i_{f0} starts flowing through their respective sequence networks with z_{g1}, z_{g2}, z_{g0} as sequence impedances of the source, and z_{line1}, z_{line2}, z_{line0}

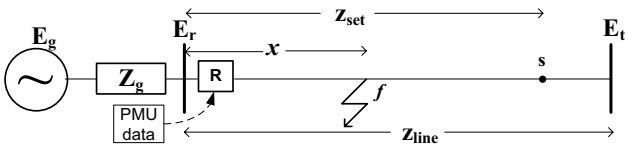

Fig. 1 Test system

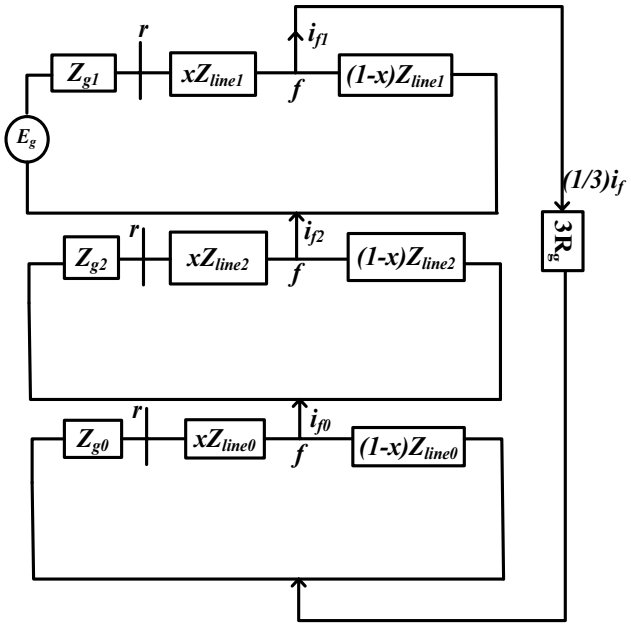

Fig. 2 Sequence network

as sequence impedances of the complete line. Parameter *x* represents the distance to the fault point from the relay end and is expressed as the percentage of the complete line length. Hence, the phase difference between the relay point voltage and fault point voltage can be given as,

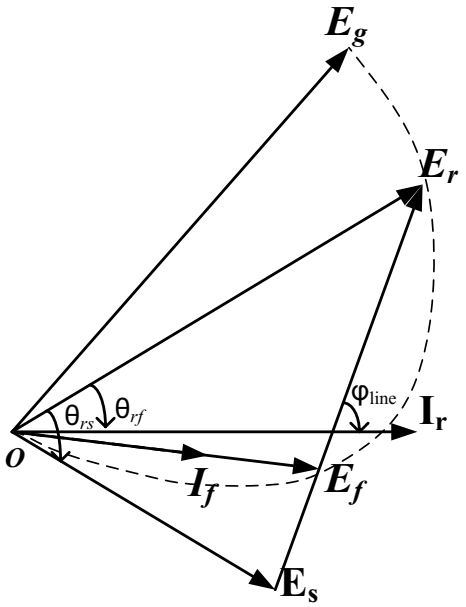

Fig. 3 Voltage phasor diagram during phase-ground fault

$$\theta_{rf} = \arg\left(\frac{\overline{E}_r}{\overline{E}_f}\right) = \arg\left(\frac{\overline{E}_r}{\overline{i}_f}\right) \quad (1)$$

As, during the fault, the phase of negative sequence current at fault point is same as that of the negative sequence current at relaying point [30] and the phase of fault current is same as that of fault point sequence current, the phase of fault point current is equivalent to that of sequence current at relaying point. So, this paper uses the phase of negative sequence (i_{r2}) current at relaying point instead of the phase of fault point current. So, the proposed method which is a phase comparison-based technique, it requires only the phases of the Relay end voltage, fault point voltage and set point voltage to be measured.

$$= \arg\left(\frac{\overline{E}_r}{\overline{i}_{r2}}\right) \quad (2)$$

Here $\overline{E}_r$ and $\overline{i}_r$ are the synchronized voltage and current phasors measured at relaying point *r*. Similarly, $\overline{E}_f$ and $\overline{i}_f$ are the fault voltage and fault current at point *f*. For different values of R_f at point *f*, $\overline{E}_f$ moves along the arc.

If $\overline{E}_s$ is the set point voltage, the phase difference between relay point voltage and set point voltage can be given as,

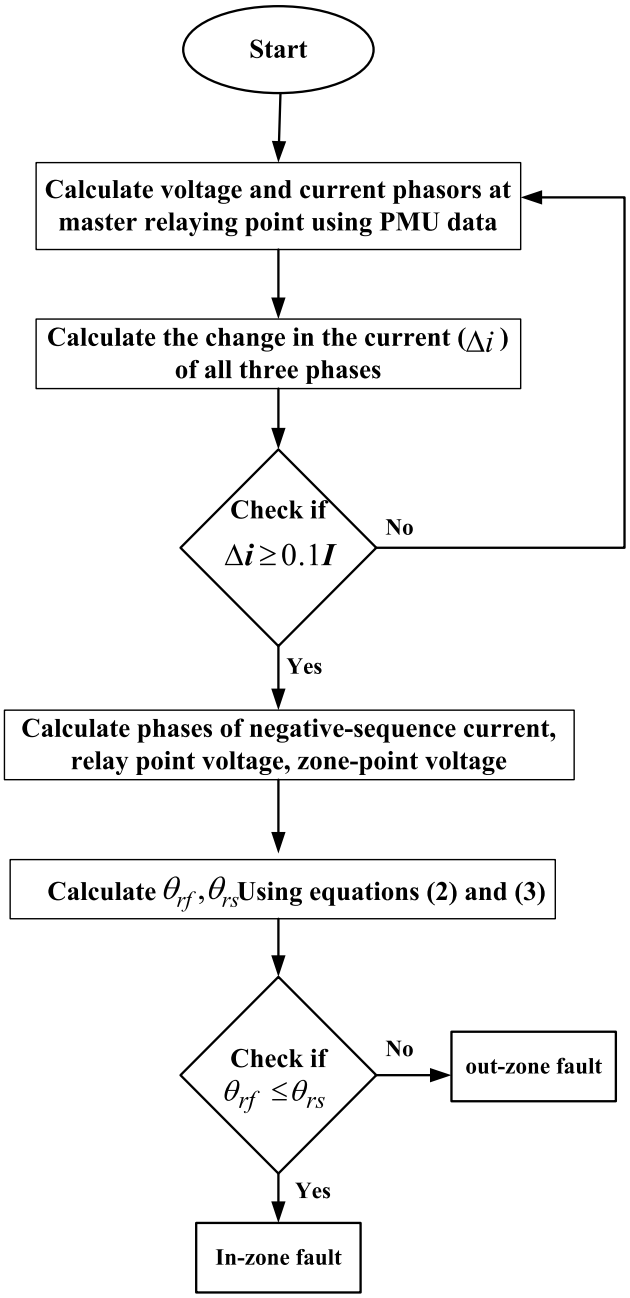

Fig. 4 Flow chart of the proposed protection scheme

Table 1 Performance of proposed methodology for the fault resistance of 100 Ω under no-load

Fault location (kms)	Time, s	θ_{rf}, deg	θ_{rs}, deg	Comparing θ_{rf} & θ_{rs}
10	0.5	7.3	0	$\theta_{rf} > \theta_{rs}$
	1	7.3	0	$\theta_{rf} > \theta_{rs}$
	1.01	7.3	0	$\theta_{rf} > \theta_{rs}$
	1.0146	0.1	2.7	$\theta_{rf} < \theta_{rs}$
	1.02	0.1	2.7	$\theta_{rf} < \theta_{rs}$
	1.03	0.1	2.7	$\theta_{rf} < \theta_{rs}$
30	0.5	7.3	0	$\theta_{rf} > \theta_{rs}$
	1	7.3	0	$\theta_{rf} > \theta_{rs}$
	1.01	7.3	0	$\theta_{rf} > \theta_{rs}$
	1.0146	6.8	8.2	$\theta_{rf} < \theta_{rs}$
	1.02	6.8	8.2	$\theta_{rf} < \theta_{rs}$
	1.03	6.8	8.2	$\theta_{rf} < \theta_{rs}$
60	0.5	7.3	0	$\theta_{rf} > \theta_{rs}$
	1	7.3	0	$\theta_{rf} > \theta_{rs}$
	1.01	7.3	0	$\theta_{rf} > \theta_{rs}$
	1.0146	14.3	16.2	$\theta_{rf} < \theta_{rs}$
	1.02	14.3	16.2	$\theta_{rf} < \theta_{rs}$
	1.03	14.3	16.2	$\theta_{rf} < \theta_{rs}$
90	0.5	7.3	0	$\theta_{rf} > \theta_{rs}$
	1	7.3	0	$\theta_{rf} > \theta_{rs}$
	1.01	7.3	0	$\theta_{rf} > \theta_{rs}$
	1.0146	20	19.1	$\theta_{rf} > \theta_{rs}$
	1.02	20	19.1	$\theta_{rf} > \theta_{rs}$
	1.03	20	19.1	$\theta_{rf} > \theta_{rs}$

Table 2 Performance of proposed methodology for the fault resistance of 1000 Ω under no-load

Fault location (kms)	Time, s	θ_{rf}, deg	θ_{rs}, deg	Comparing θ_{rf} & θ_{rs}
10	0.5	7.3	0	$\theta_{rf} > \theta_{rs}$
	1	7.3	0	$\theta_{rf} > \theta_{rs}$
	1.01	7.3	0	$\theta_{rf} > \theta_{rs}$
	1.0146	1.8	3	$\theta_{rf} < \theta_{rs}$
	1.02	1.8	3	$\theta_{rf} < \theta_{rs}$
	1.03	1.8	3	$\theta_{rf} < \theta_{rs}$
30	0.5	7.3	0	$\theta_{rf} > \theta_{rs}$
	1	7.3	0	$\theta_{rf} > \theta_{rs}$
	1.01	7.3	0	$\theta_{rf} > \theta_{rs}$
	1.0146	7.6	8.4	$\theta_{rf} < \theta_{rs}$
	1.02	7.6	8.4	$\theta_{rf} < \theta_{rs}$
	1.03	7.6	8.4	$\theta_{rf} < \theta_{rs}$
60	0.5	7.3	0	$\theta_{rf} > \theta_{rs}$
	1	7.3	0	$\theta_{rf} > \theta_{rs}$
	1.01	7.3	0	$\theta_{rf} > \theta_{rs}$
	1.0146	16	16.3	$\theta_{rf} < \theta_{rs}$
	1.02	16	16.3	$\theta_{rf} < \theta_{rs}$
	1.03	16	16.3	$\theta_{rf} < \theta_{rs}$
90	0.5	8.6	0	$\theta_{rf} > \theta_{rs}$
	1	8.6	0	$\theta_{rf} > \theta_{rs}$
	1.01	8.6	0	$\theta_{rf} > \theta_{rs}$
	1.0146	21	19	$\theta_{rf} > \theta_{rs}$
	1.02	21	19	$\theta_{rf} > \theta_{rs}$
	1.03	21	19	$\theta_{rf} > \theta_{rs}$

Table 3 Performance of proposed methodology for the fault resistance of 100 Ω under RL-load, with r-side phase angle of 30°

Fault location (kms)	Time, s	θ_{rf}, deg	θ_{rs}, deg	Comparing θ_{rf} & θ_{rs}
10	0.5	209	34	$\theta_{rf} > \theta_{rs}$
	1	209	34	$\theta_{rf} > \theta_{rs}$
	1.01	209	34	$\theta_{rf} > \theta_{rs}$
	1.0146	0	35	$\theta_{rf} < \theta_{rs}$
	1.02	0	35	$\theta_{rf} < \theta_{rs}$
	1.03	0	35	$\theta_{rf} < \theta_{rs}$
30	0.5	199	32	$\theta_{rf} > \theta_{rs}$
	1	199	32	$\theta_{rf} > \theta_{rs}$
	1.01	199	32	$\theta_{rf} > \theta_{rs}$
	1.0146	11	38	$\theta_{rf} < \theta_{rs}$
	1.02	11	38	$\theta_{rf} < \theta_{rs}$
	1.03	11	38	$\theta_{rf} < \theta_{rs}$
60	0.5	199	32	$\theta_{rf} > \theta_{rs}$
	1	199	32	$\theta_{rf} > \theta_{rs}$
	1.01	199	32	$\theta_{rf} > \theta_{rs}$
	1.0146	30	40	$\theta_{rf} < \theta_{rs}$
	1.02	30	40	$\theta_{rf} < \theta_{rs}$
	1.03	30	40	$\theta_{rf} < \theta_{rs}$
90	0.5	199	32	$\theta_{rf} > \theta_{rs}$
	1	199	32	$\theta_{rf} > \theta_{rs}$
	1.01	199	32	$\theta_{rf} > \theta_{rs}$
	1.0146	137	34	$\theta_{rf} > \theta_{rs}$
	1.02	137	34	$\theta_{rf} > \theta_{rs}$
	1.03	137	34	$\theta_{rf} > \theta_{rs}$

$$\theta_{rs} = \arg\left(\frac{\overline{E}_r}{\overline{E}_s}\right) \tag{3}$$

where

$$\overline{E}_s = (\overline{E}_r - \bar{i}_r.z_{set}) \tag{4}$$

So,

$$\theta_{rs} = \arg\left(\frac{\overline{E}_r}{(\overline{E}_r - \bar{i}_r.z_{set})}\right) \tag{5}$$

2.2 Double-Sourced System

In a double-sourced system, if a single phase to ground fault occurs, the fault point voltage $\overline{E}_f$ lags behind $\bar{i}_r$. This is due to the contribution of current from the other source. This causes an angular difference between $\bar{i}_r$ and $\overline{\text{i}}_\text{f}$ $\bar{i}_f$. Now, the phase difference between the relay point voltage, $\overline{\text{Er}}$ $\overline{E}_r$ and fault point voltage, $\overline{E}_f$ becomes,

$$\begin{aligned} &= \arg\left(\frac{\overline{E}_r}{\bar{i}_r}\right) + \arg\left(\frac{\bar{i}_r}{\bar{i}_f}\right) \\ &= \arg\left(\frac{\overline{E}_r}{\bar{i}_r}\right) + \arg\left(\frac{\bar{i}_r}{\bar{i}_{r2}}\right) \end{aligned} \tag{6}$$

It says that the effect of load/source current from the sond source will be accounted by means of the sond term in the above Eq. (6).

3 Condition for Fault Detection

Under the no-load condition, when a single-phase to ground fault occurs in between relay point and set-point, the position of fault current phasor $\overline{\text{i}}_\text{f}$ $\bar{i}_f$ will be same as relay point current phasor $\overline{\text{i}}_\text{r}$ $\bar{i}_r$. Hence, unlike in Fig. 3, the phasor $\overline{E}_f$ will be in-phase with $\overline{\text{i}}_\text{r}$ $\bar{i}_r$. Then the estimated set point voltage $\overline{\text{E}}_\text{s}$ $\overline{E}_s$ will lag behind $\overline{\text{i}}_\text{r}$ $\bar{i}_r$. But under loaded condition, the phasor $\overline{E}_f$ lags behind $\overline{\text{i}}_\text{r}$ $\bar{i}_r$. As shown in Fig. 3, whenever a single-phase to ground fault occurs at point *f*, then the fault

Table 4 Performance of proposed methodology for the fault resistance of 500 Ω under RL-load, with r-side phase angle of 30°

Fault location (kms)	Time, s	θ_{rf}, deg	θ_{rs}, deg	Comparing θ_{rf} & θ_{rs}
10	0.5	209	34	$\theta_{rf} > \theta_{rs}$
	1	209	34	$\theta_{rf} > \theta_{rs}$
	1.01	209	34	$\theta_{rf} > \theta_{rs}$
	1.0146	29	34	$\theta_{rf} < \theta_{rs}$
	1.02	29	34	$\theta_{rf} < \theta_{rs}$
	1.03	29	34	$\theta_{rf} < \theta_{rs}$
30	0.5	199	31	$\theta_{rf} > \theta_{rs}$
	1	199	31	$\theta_{rf} > \theta_{rs}$
	1.01	199	31	$\theta_{rf} > \theta_{rs}$
	1.0146	19	31	$\theta_{rf} < \theta_{rs}$
	1.02	19	31	$\theta_{rf} < \theta_{rs}$
	1.03	19	31	$\theta_{rf} < \theta_{rs}$
60	0.5	199	31	$\theta_{rf} > \theta_{rs}$
	1	199	31	$\theta_{rf} > \theta_{rs}$
	1.01	199	31	$\theta_{rf} > \theta_{rs}$
	1.0146	20	31	$\theta_{rf} < \theta_{rs}$
	1.02	20	31	$\theta_{rf} < \theta_{rs}$
	1.03	20	31	$\theta_{rf} < \theta_{rs}$
90	0.5	199	31	$\theta_{rf} > \theta_{rs}$
	1	199	31	$\theta_{rf} > \theta_{rs}$
	1.01	199	31	$\theta_{rf} > \theta_{rs}$
	1.0146	68	31	$\theta_{rf} > \theta_{rs}$
	1.02	68	31	$\theta_{rf} > \theta_{rs}$
	1.03	68	31	$\theta_{rf} > \theta_{rs}$

voltage lags immediately behind the relay point voltage $\overline{E}_r$. So, the condition for the existence of fault inside set point *s* is,

$$\theta_{rf} \leq \theta_{rs} \tag{7}$$

If the fault is beyond the set point, then $\overline{E}_f$ lags immediately behind the set point voltage $\overline{E}_s$. So, the condition becomes,

$$\theta_{rf} > \theta_{rs} \tag{8}$$

Finally, the fault protection criterion is as given below:

Condition 1: $\theta_{\leq \theta rf\, r,}$ *if fault is in-between relay and set points*

Condition 2: $\theta_{> \theta rf\, r,}$ *if fault is beyond set points*

4 Results and Discussions

The simulation was carried out in EMTDC/PSCAD environment. The detailed parameters for the simulated system model are given below.

Table 5 Performance of proposed methodology for the fault resistance of 100 Ω under RL-load, with r-side phase angle of 30°, fault inception angle of 15°

Fault location (kms)	Time, s	θ_{rf}, deg	θ_{rs}, deg	Comparing θ_{rf} & θ_{rs}
10	0.5	208	34	$\theta_{rf} > \theta_{rs}$
	1	208	34	$\theta_{rf} > \theta_{rs}$
	1.01	208	34	$\theta_{rf} > \theta_{rs}$
	1.0146	0	36	$\theta_{rf} < \theta_{rs}$
	1.02	0	36	$\theta_{rf} < \theta_{rs}$
	1.03	0	36	$\theta_{rf} < \theta_{rs}$
30	0.5	199	31	$\theta_{rf} > \theta_{rs}$
	1	199	31	$\theta_{rf} > \theta_{rs}$
	1.01	199	31	$\theta_{rf} > \theta_{rs}$
	1.0146	18	35	$\theta_{rf} < \theta_{rs}$
	1.02	18	35	$\theta_{rf} < \theta_{rs}$
	1.03	18	35	$\theta_{rf} < \theta_{rs}$
60	0.5	199	31	$\theta_{rf} > \theta_{rs}$
	1	199	31	$\theta_{rf} > \theta_{rs}$
	1.01	199	31	$\theta_{rf} > \theta_{rs}$
	1.0146	30	41	$\theta_{rf} < \theta_{rs}$
	1.02	30	41	$\theta_{rf} < \theta_{rs}$
	1.03	30	41	$\theta_{rf} < \theta_{rs}$
90	0.5	199	31	$\theta_{rf} > \theta_{rs}$
	1	199	31	$\theta_{rf} > \theta_{rs}$
	1.01	199	31	$\theta_{rf} > \theta_{rs}$
	1.0146	68	33	$\theta_{rf} > \theta_{rs}$
	1.02	68	33	$\theta_{rf} > \theta_{rs}$
	1.03	68	33	$\theta_{rf} > \theta_{rs}$

Source impedance: 0.1 Ω,
TLine model: frequency dependent (phase) model,
Voltage: 230 kV,
Line length: 100 km,
Tower: 3L1,
Conductor name: chukar,
Conductor_configuration: 3wire, unsymmetrical,
Height of conductor: 30 m,
Horizontal spacing between conductors: 10 m,
Conductor_radius: 0.0203454 m,
Line_resistance: 0.140696 E-03 [ohm/m],
Line_reactance: 0.783171 E-03 [ohm/m],
Shunt_conductance: 1.0E-11 [mho/m].

The proposed scheme, as described in Fig. 4, after calculating the synchronized voltage and current phasors at the master relay point, it determines the change in current. Based on the tolerance value it calculates the phase angles of the negative sequence current, relay point voltage and zone-point voltage. Then, it identifies the existence of zone fault. The fault is simulated at 1 s. The zone is selected as 80 kms of the line *rt.*

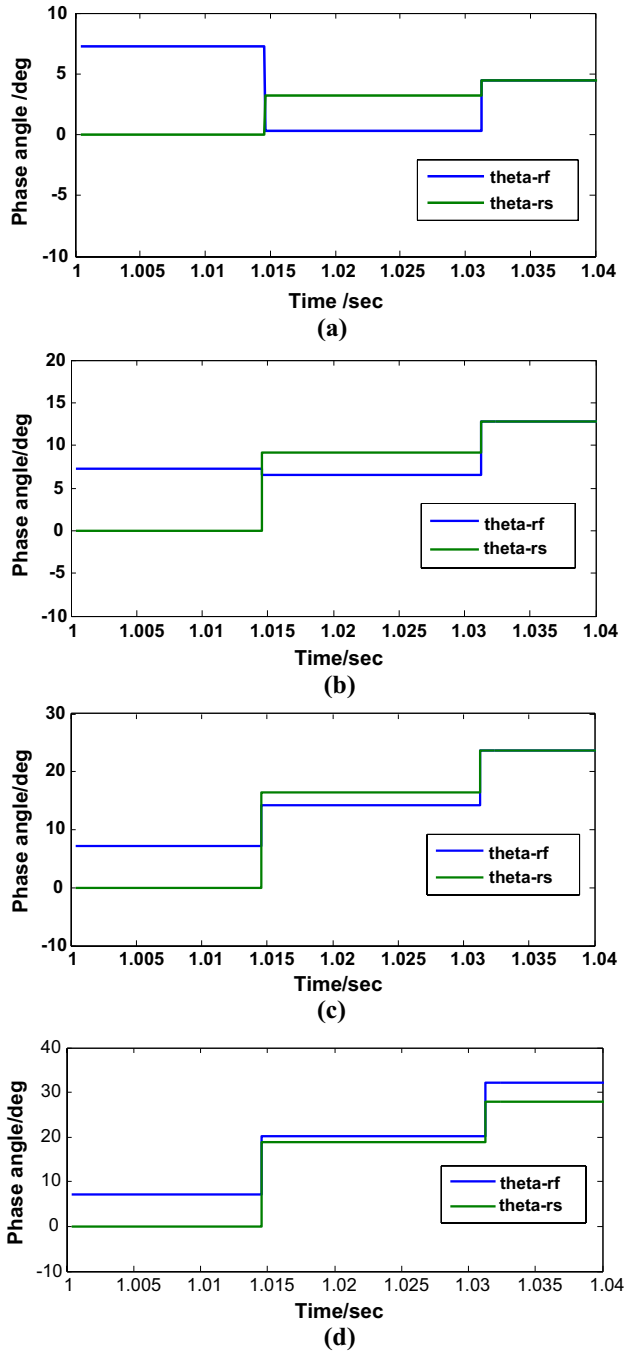

Fig. 5 Results for No-load and 100 Ω fault resistance at **a** 10 kms, **b** 30 kms, **c** 60 kms, **d** 90 kms

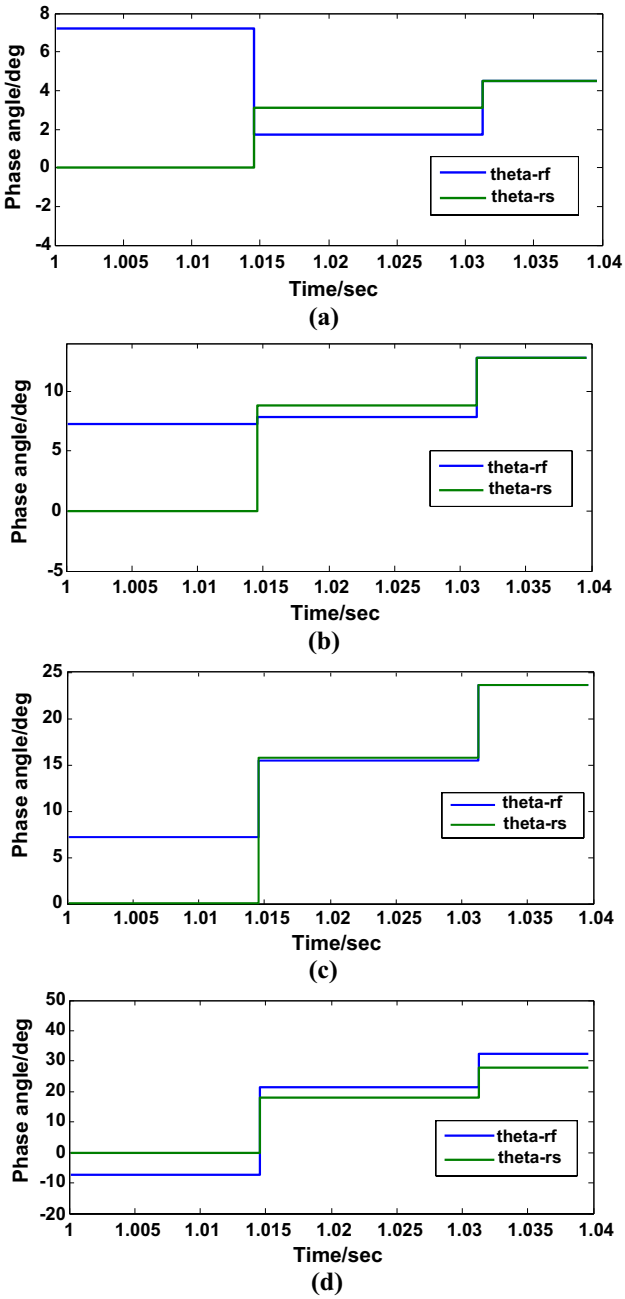

Fig. 6 Results for No-load and 1000 Ω fault resistance at **a** 10 kms, **b** 30 kms, **c** 60 kms, **d** 90 kms

4.1 Under Different Fault Resistances

The increase in fault resistance makes the relay to be under reach. It also affects the directional feature of mho relay. This effect may be less significant if the fault location comes closer to relay point. At a certain value of fault resistance, some of the mho elements become non- directional.

For a single phase-ground fault at different locations in the line *rt*, the simulation results obtained for different fault resistances under different system conditions are presented below. Under no-load, the fault identification results for different fault resistances at different locations considering phase angle variations at end *r* are given in Tables 1 and 2. The simulation results considering RL-load are given in Tables 3, 4 and 5. From the tables, it is understood that whenever fault lies after 80 kms (which is the set point for

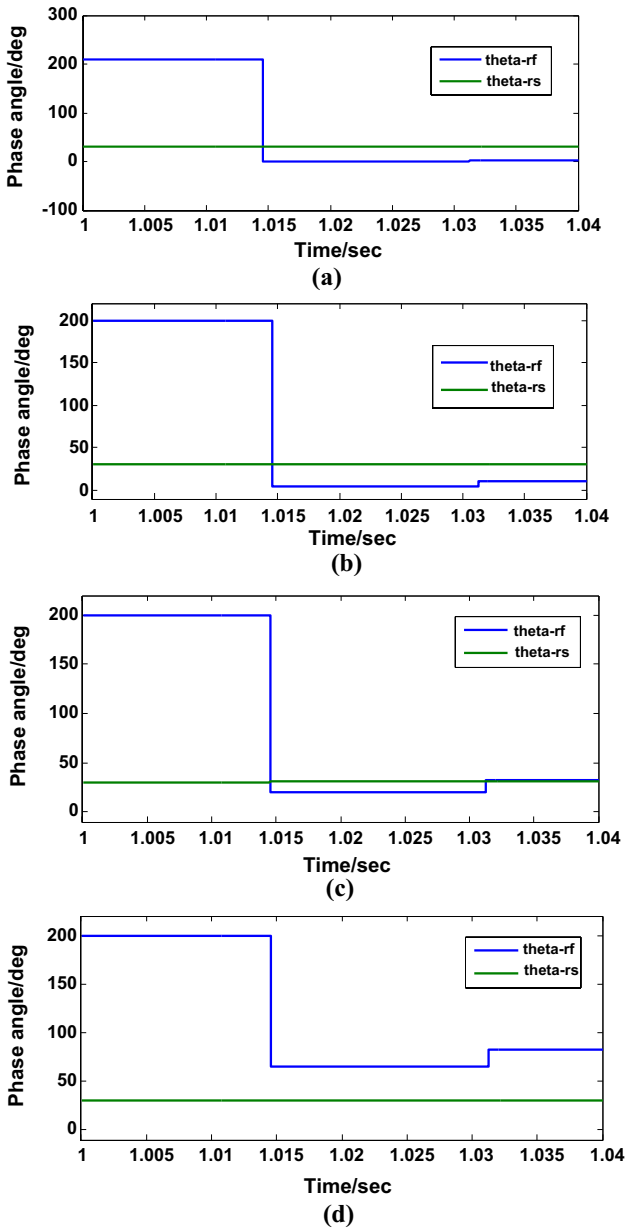

Fig. 7 Results for RL-load and 1000 Ω fault resistance at **a** 10 kms, **b** 30 kms, **c** 60 kms, **d** 90 kms

the zone), the phase difference between the relay point voltage and fault point voltage (θ_{rf}) is becoming greater than the phase difference between relay point voltage and set point voltage (θ_{rs}). The correctness of the suggested technique can be seen from Figs. 5, 6 and 7. These results show that the algorithm identifies the fault within 14.6 ms irrespective of the fault resistance.

As the occurrence of the fault is to be checked, the condition $\Delta i \geq 0.1I$ is checked first. Here, Δi is the jump in the current sampling, $0.1I$ is the threshold value of the current jump.

Table 6 Performance of proposed methodology for the double sourced system with fault resistance of 100 Ω, with r-side phase angle of − 20°

Fault location (kms)	Time, s	θ_{rf}, deg	θ_{rs}, deg	Comparing θ_{rf} & θ_{rs}
10	0.5	39.5	16	$\theta_{rf} > \theta_{rs}$
	1	39.5	16	$\theta_{rf} > \theta_{rs}$
	1.01	39.5	16	$\theta_{rf} > \theta_{rs}$
	1.0146	4	16.5	$\theta_{rf} < \theta_{rs}$
	1.02	4	16.5	$\theta_{rf} < \theta_{rs}$
	1.03	4	16.5	$\theta_{rf} < \theta_{rs}$
30	0.5	29.5	5.2	$\theta_{rf} > \theta_{rs}$
	1	29.5	5.2	$\theta_{rf} > \theta_{rs}$
	1.01	29.5	5.2	$\theta_{rf} > \theta_{rs}$
	1.0146	−10	0	$\theta_{rf} < \theta_{rs}$
	1.02	−10	0	$\theta_{rf} < \theta_{rs}$
	1.03	−10	0	$\theta_{rf} < \theta_{rs}$
60	0.5	36	12	$\theta_{rf} > \theta_{rs}$
	1	36	12	$\theta_{rf} > \theta_{rs}$
	1.01	36	12	$\theta_{rf} > \theta_{rs}$
	1.0146	−8	4	$\theta_{rf} < \theta_{rs}$
	1.02	−8	4	$\theta_{rf} < \theta_{rs}$
	1.03	−8	4	$\theta_{rf} < \theta_{rs}$
90	0.5	23	−16	$\theta_{rf} > \theta_{rs}$
	1	23	−16	$\theta_{rf} > \theta_{rs}$
	1.01	23	−16	$\theta_{rf} > \theta_{rs}$
	1.0146	−13.5	−14	$\theta_{rf} > \theta_{rs}$
	1.02	−13.5	−14	$\theta_{rf} > \theta_{rs}$
	1.03	−13.5	−14	$\theta_{rf} > \theta_{rs}$

4.2 Under Different Fault Resistances Considering Double-Sourced System

If the angle $\delta = +10^0$, the line end r becomes sending end, and for $\delta = -10^0$ the same end becomes receiving end. Line loading depends on the phasor difference between the two line ends. More the phasor difference heavily loaded the line is. Tables 6, 7, 8 and 9 gives the performance of the proposed algorithm considering a double-sourced system under

Table 7 Performance of proposed methodology for the double sourced system with fault resistance of 100 Ω, with r-side phase angle of 20°

Fault location (kms)	Time, s	θ_{rf}, deg	θ_{rs}, deg	Comparing θ_{rf} & θ_{rs}
10	0.5	136	20	$\theta_{rf} > \theta_{rs}$
	1	136	20	$\theta_{rf} > \theta_{rs}$
	1.01	136	20	$\theta_{rf} > \theta_{rs}$
	1.0146	−4	17	$\theta_{rf} < \theta_{rs}$
	1.02	−4	17	$\theta_{rf} < \theta_{rs}$
	1.03	−4	17	$\theta_{rf} < \theta_{rs}$
30	0.5	136	20	$\theta_{rf} > \theta_{rs}$
	1	136	20	$\theta_{rf} > \theta_{rs}$
	1.01	136	20	$\theta_{rf} > \theta_{rs}$
	1.0146	6	24	$\theta_{rf} < \theta_{rs}$
	1.02	6	24	$\theta_{rf} < \theta_{rs}$
	1.03	6	24	$\theta_{rf} < \theta_{rs}$
60	0.5	136	20	$\theta_{rf} > \theta_{rs}$
	1	136	20	$\theta_{rf} > \theta_{rs}$
	1.01	136	20	$\theta_{rf} > \theta_{rs}$
	1.0146	8	22	$\theta_{rf} < \theta_{rs}$
	1.02	8	22	$\theta_{rf} < \theta_{rs}$
	1.03	8	22	$\theta_{rf} < \theta_{rs}$
90	0.5	136	20	$\theta_{rf} > \theta_{rs}$
	1	136	20	$\theta_{rf} > \theta_{rs}$
	1.01	136	20	$\theta_{rf} > \theta_{rs}$
	1.0146	24	22	$\theta_{rf} > \theta_{rs}$
	1.02	24	22	$\theta_{rf} > \theta_{rs}$
	1.03	24	22	$\theta_{rf} > \theta_{rs}$

Table 8 Performance of proposed methodology for the double sourced system with fault resistance of 500 Ω, with r-side phase angle of − 20°

Fault location (kms)	Time, s	θ_{rf}, deg	θ_{rs}, deg	Comparing θ_{rf} & θ_{rs}
10	0.5	37	16	$\theta_{rf} > \theta_{rs}$
	1	37	16	$\theta_{rf} > \theta_{rs}$
	1.01	37	16	$\theta_{rf} > \theta_{rs}$
	1.0146	3	15.5	$\theta_{rf} < \theta_{rs}$
	1.02	3	15.5	$\theta_{rf} < \theta_{rs}$
	1.03	3	15.5	$\theta_{rf} < \theta_{rs}$
30	0.5	38.5	16	$\theta_{rf} > \theta_{rs}$
	1	38.5	16	$\theta_{rf} > \theta_{rs}$
	1.01	38.5	16	$\theta_{rf} > \theta_{rs}$
	1.0146	0	15	$\theta_{rf} < \theta_{rs}$
	1.02	0	15	$\theta_{rf} < \theta_{rs}$
	1.03	0	15	$\theta_{rf} < \theta_{rs}$
60	0.5	39	16	$\theta_{rf} > \theta_{rs}$
	1	39	16	$\theta_{rf} > \theta_{rs}$
	1.01	39	16	$\theta_{rf} > \theta_{rs}$
	1.0146	−4	14	$\theta_{rf} < \theta_{rs}$
	1.02	−4	14	$\theta_{rf} < \theta_{rs}$
	1.03	−4	14	$\theta_{rf} < \theta_{rs}$
90	0.5	23.5	−16	$\theta_{rf} > \theta_{rs}$
	1	23.5	−16	$\theta_{rf} > \theta_{rs}$
	1.01	23.5	−16	$\theta_{rf} > \theta_{rs}$
	1.0146	−15	−15.5	$\theta_{rf} > \theta_{rs}$
	1.02	−15	−15.5	$\theta_{rf} > \theta_{rs}$
	1.03	−15	−15.5	$\theta_{rf} > \theta_{rs}$

different fault resistances and system conditions. From the Figs. 8 and 9, it is clear that the proposed algorithm could detect the fault in any double-sourced system independently with the fault resistance.

4.3 Under Different Fault Resistances Considering Double-Sourced System and Fault Inception

The worst fault-induced transient condition in both voltages and currents in SLG faults corresponds to the fault striking in the voltage peak. The fault-induced transients are more severe for the fault inception angles 30^0, 90^0 and 150^0. As, the severity of fault-induced transients depends on point of fault striking in the voltage peak and the Synchronized phasor data is an accurate measure of the phase information of the voltage wave, the proposed phase-angle based fault detection algorithm detects the fault independently with fault-inception angle under any fault resistances. The accuracy of this technique for different fault resistances considering fault-inception at 15^0 is given in Fig. 10.

Since the distance protection is highly sensitive to the fault and/or source impedance, it may either not operate for the faults within the zone of protection or mal-operate for the faults outside zone. But, the proposed method makes, if it is applied in-conjunction with distance relay, the distance protection scheme immune to the source and/or fault resistance.

5 Conclusion

In this paper, a novel scheme of voltage phase comparison based single line-ground fault detection is proposed based on synchronized phasor data. The simulation results mean that the proposed scheme has following advantages:

Table 9 Performance of proposed methodology for the double sourced system with fault resistance of 500 Ω, with r-side phase angle of 20°

Fault location (kms)	Time, s	θ_{rf}, deg	θ_{rs}, deg	Comparing θ_{rf} & θ_{rs}
10	0.5	136	16	$\theta_{rf} > \theta_{rs}$
	1	136	16	$\theta_{rf} > \theta_{rs}$
	1.01	136	16	$\theta_{rf} > \theta_{rs}$
	1.0146	−7	16	$\theta_{rf} < \theta_{rs}$
	1.02	−7	16	$\theta_{rf} < \theta_{rs}$
	1.03	−7	16	$\theta_{rf} < \theta_{rs}$
30	0.5	135	16	$\theta_{rf} > \theta_{rs}$
	1	135	16	$\theta_{rf} > \theta_{rs}$
	1.01	135	16	$\theta_{rf} > \theta_{rs}$
	1.0146	−4	17	$\theta_{rf} < \theta_{rs}$
	1.02	−4	17	$\theta_{rf} < \theta_{rs}$
	1.03	−4	17	$\theta_{rf} < \theta_{rs}$
60	0.5	135	16	$\theta_{rf} > \theta_{rs}$
	1	135	16	$\theta_{rf} > \theta_{rs}$
	1.01	135	16	$\theta_{rf} > \theta_{rs}$
	1.0146	4	18	$\theta_{rf} < \theta_{rs}$
	1.02	4	18	$\theta_{rf} < \theta_{rs}$
	1.03	4	18	$\theta_{rf} < \theta_{rs}$
90	0.5	136	20	$\theta_{rf} > \theta_{rs}$
	1	136	20	$\theta_{rf} > \theta_{rs}$
	1.01	136	20	$\theta_{rf} > \theta_{rs}$
	1.0146	23	21	$\theta_{rf} > \theta_{rs}$
	1.02	23	21	$\theta_{rf} > \theta_{rs}$
	1.03	23	21	$\theta_{rf} > \theta_{rs}$

It is highly immune to fault resistance. It differentiates the in-zone fault from out-zone faults irrespective of fault resistance. So, the problem of relay mal-operation caused by fault resistance is answered.

The fault identification is unaffected by the system operation and load conditions. It means the algorithm works satisfactorily under any load and/or power flow direction.

Finally, the reduction in the time of fault identification significantly improves the transient stability of the system. It is highly significant in power system protection practices.

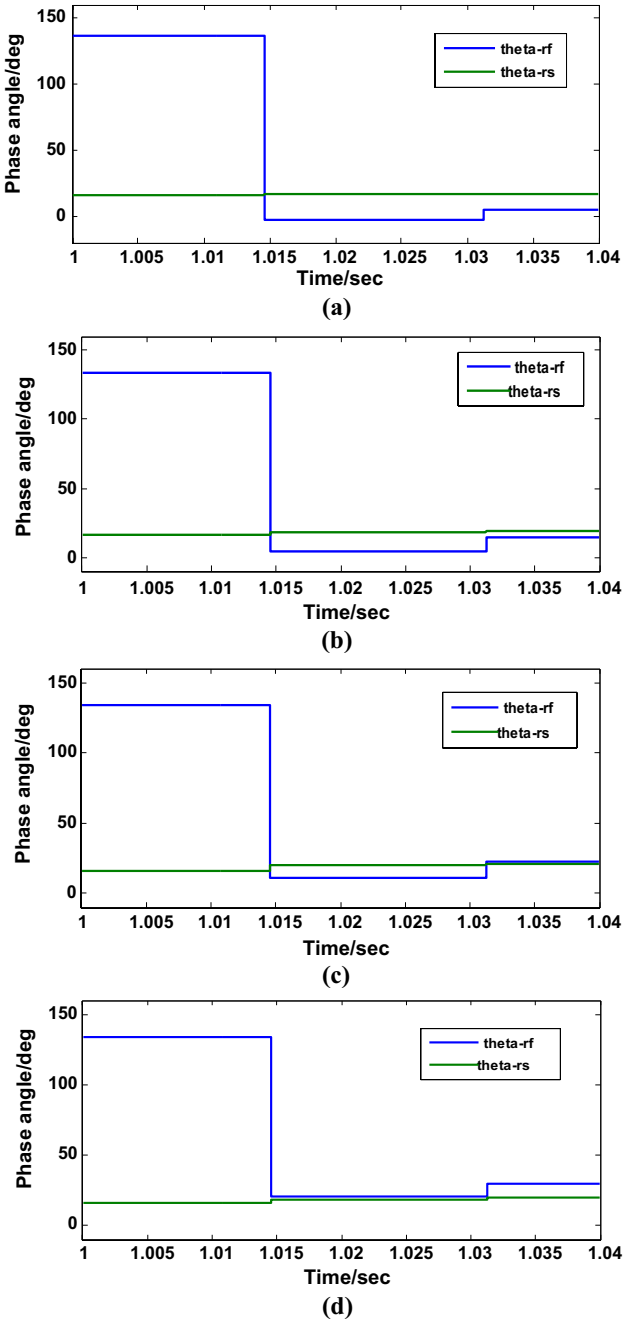

Fig. 8 Results for Double-sourced, 100 Ω fault resistance and $\delta_1 = 20^0$, $\delta_2 = 0^0$ at **a** 10 kms, **b** 30 kms, **c** 60 kms, **d** 90 kms

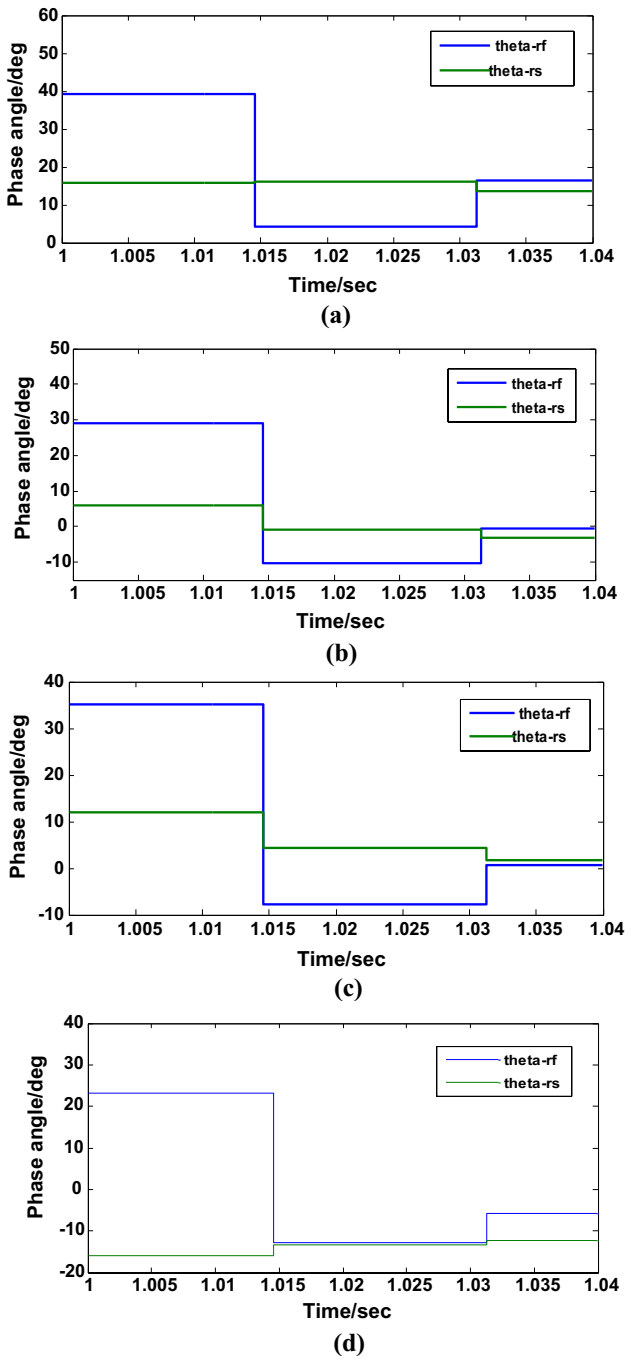

Fig. 9 Results for Double-sourced, 100 Ω fault resistance and $\delta_1 = -20^0$, $\delta_2 = 20^0$ at **a** 10 kms, **b** 30 kms, **c** 60 kms, **d** 90 kms

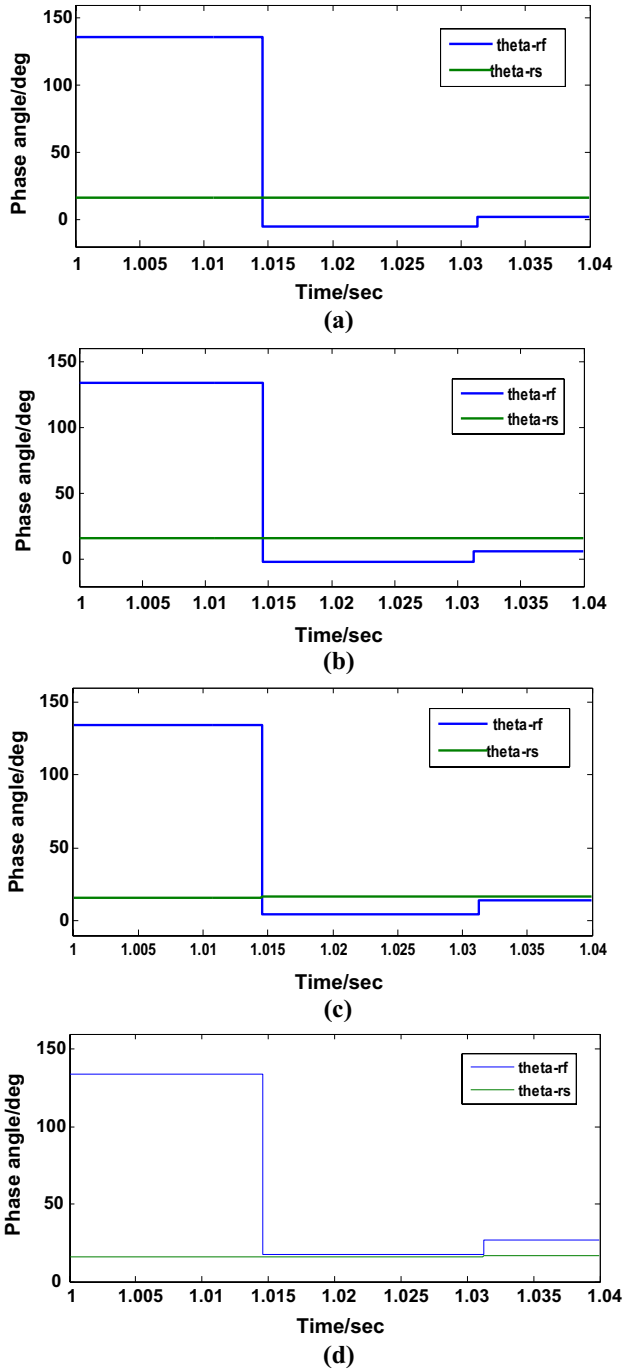

Fig. 10 Results for Double-sourced, 100 Ω fault resistance, Fault inception angle: 15^0 and $\delta_1 = 20^0$, $\delta_2 = 0^0$ at **a** 10 kms, **b** 30 kms, **c** 60 kms, **d** 90 kms

References

1. Working Group H-7 of the Relaying channels (1994) Synchronized sampling and phasor measurements for relaying and control. IEEE Trans Power Deliv vol 9, no. 1, pp 442–452
2. Jiang J-A, Yang J-Z, Lin Y-H, Liu C-W, Ma J-C (Apr.2000) An adaptive PMU based fault detection/location technique for transmission lines, Part I: Theory and algorithms. IEEE Trans Power Deliv 15:486–493
3. Jiang J-A, Lin Y-H, Yang J-Z, Too T-M, Liu C-W (2000) An adaptive PMU based fault detection/location technique for transmission lines, Part II: PMU implementation and performance evaluation. IEEE Trans Power Del 15:1136–1146
4. Jiang JA, Chen C-S, Liu C-W (2003) A new protection scheme for fault detection, direction discrimination, classification and location in transmission lines. IEEE Trans. Power Deliv 17(1):34–42

5. Bo W, Jiang Q, Cao Y (2009) Transmission network fault location using sparse PMU measurements. Int Conf Sustain Power Gener Supply 2009:1–6
6. Lien K, Liu C, Yu C, Jiang J (2006) Transmission network fault location observability with minimal PMU placement. IEEE Trans Power Deliv 21(3):1128–1136
7. Shiroei M, Daniar S, Akhbari M (2009) A new algorithm for fault location on transmission lines. In: IEEE Power and Energy Society General Meeting, pp 1–5
8. Geramian SS, Abyane HA, Mazlumi K (2008) Determination of optimal PMU placement for fault location using genetic algorithm. In: 13th international conference on harmonics and quality of power, pp 1–5
9. Mazlumi K, Abyaneh HA, Sadeghi SH, Geramian SS (2008) Determination of optimal PMU placement for fault-location observability. In: Third international conference on electric utility deregulation and restructuring and power technologies, pp 1938–1942
10. Chuang CL, Jiang JA, Wang YC, Chen CP, Hsiao YT (2007) An adaptive PMU-based fault location estimation system with a fault-tolerance and load-balancing communication network. In: IEEE Lausanne Power Tech, pp 1197–1202
11. Lin Y, Liu C, Chen C (2004) A new PMU-based fault detection/location technique for transmission lines with consideration of arcing fault discrimination-Part I: theory and algorithms. IEEE Trans Power Deliv 19(4):1587–1593
12. Lin Y, Liu C, Chen C (2004) A new PMU-based fault detection/location technique for transmission lines with consideration of arcing fault discrimination—Part II: performance evaluation. IEEE Trans Power Del 19(4):1594–1601
13. Gu JC, Yu SL (2000) Removal of DC offset in current and voltage signals using a novel Fourier filter algorithm. IEEE Trans Power Deliv 15(1):73–79
14. Guo Y, Kezunovic M, Chen D (2003) Simplified algorithms for removal of the effect of exponentially decaying DC-offset on the Fourier algorithm. IEEE Trans Power Del 18(3):711–717
15. Nam S-R, Park J-Y, Kang S-H, Kezunovic M (2009) Phasor estimation in the presence of DC offset and CT saturation. IEEE Trans Power Del 24(4):1842–1849
16. Benmouyal G (1995) Removal of DC-offset in current waveforms using digital mimic filtering. IEEE Trans Power Del 10(2):621–630
17. Kang S-H, Lee D-G, Nam S-R, Crossley PA, Kang Y-C (2009) Fourier transform-based modified phasor estimation method immune to the effect of the DC offsets. IEEE Trans Power Del 24(3):1104–1111
18. Mai RK, Fu L, Dong ZY, Kirby B, Bo ZQ (2011) An adaptive dynamic phasor estimator considering DC offset for PMU applications. IEEE Trans Power Del 26(3):1744–1754
19. Eissa MM (2006) Ground distance relay compensation based on fault resistance calculation. IEEE Trans Power Del 21(4):1830–1835
20. Filomena AD, Salim RH, Resener M, Bretas AS (2008) Ground distance relaying with fault-resistance compensation for unbalanced systems. IEEE Trans Power Del 23(3):1319–1326
21. Miao S, Liu P, Lin X (2010) An adaptive operating characteristic toimprove the operation stability of percentage differential protection. IEEE Trans Power Del 25(3):1410–1417
22. Xianguo J, Zengping W, Zhichao Z et al (2013) Single-phase high resistance fault protection based on active power of fault resistance. Proc CSEE 33(13):187–193
23. Song GB, Chu X, Gao SP et al (2013) Novel line protection based on distributed parameter model for long-distance transmission lines. IEEE Trans Power Del 28(4):2116–2123
24. Seyedi H, Teimourzadeh S, Soleiman Nezhad P (2014) Adaptive zero sequence compensation algorithm for double-circuit transmission line protection. IET Gener Trans Distrib 8(6):1107–1116
25. Ma J, Yan X, Fan B, Liu C, Thorp JS (2015) A novel line protection scheme for a single phase-to-ground fault based on voltage phase comparison. IEEE Trans Power Deliv 31(5):2018–2027
26. Babu NP, Babu PS, Sarma DS (2015) A wide-area prospective on power system protection: a state-of-art. In: 2015 International conference on energy, power and environment: towards sustainable growth (ICEPE). IEEE
27. Babu NP, Babu PS, Sarma DS (2015) A reliable wide-area measurement system using hybrid genetic particle swarm optimization (HGPSO). Int Rev Electr Eng 10(6):747–763
28. Babu NP, Babu PS, Sarma DS (2017) A new power system restoration technique based on WAMS partitioning. Eng Technol Appl Sci Res 7(4):1811–1819
29. Priyadarshini S, Panigrahi CK (2020) Optimal allocation of synchrophasor units in the distribution network considering maximum redundancy. Eng Technol Appl Sci Res 10(6):6494–6499
30. Zhu SS (2005) The theory and technology of power system relay protection, 3rd edn. China Power Press, Beijing

N. V. Phanendra Babu is currently working as an Assistant Professor in Department of Electrical and Electronics Engineering, CBIT, Hyderabad, India. His areas of interest are Optimal PMU Placement, Design of Wide-Area Measurement system and its applications.

P. Suresh Babu is currently working as an Associate Professor in Department of Electrical Engineering, NIT Warangal, India. His areas of interest are Power System Protection with digital multifunction relays, Development of Adaptive protection schemes and Digital filtering algorithms.

Saptarshi Roy is currently working as an Assistant Professor in Department of Electrical and Electronics Engineering, MMG Polytechnic college, West Bengal, India. His areas of interest are power system protection, Phasor Measurement Unit applications in power systems, Synchrophasors applications in power systems.

T. Sudhakar Babu is currently working as an Associate Professor with the Department of Electrical and Electronics Engineering, CBIT, Hyderabad, India. His research interests include design and implementation of solar PV systems, power management for hybrid energy systems, storagesystems, fuel cell technologies, electric vehicle, and smart grid.

Anil Bharadwaj is currently pursuing PhD at the Department of Electrical Engineering, IIT Kharagpur, India. Hisareas of interests are modular multilevel converters, and their applications for STATCOM with energy storage system.